Structural Engineering and Mechanics, Vol. 12, No. 5 (2001) 491-506
DOI: http://dx.doi.org/10.12989/sem.2001.12.5.491

A new piezoelectric shell element and its application in static shape control

Su Huan Chen†, Guo Feng Yao‡ and Hua Dong Lian‡†

Department of Mechanics, Jilin University, Nan-Ling Campus, Chang Chun, Jilin 130025, China

Abstract. In this paper, a new three-dimensional piezoelectric thin shell element containing an integrated distributed piezoelectric sensor and actuator is proposed. The distributed piezoelectric sensor layer monitors the structural shape deformation due to the direct effect and the distributed actuator layer suppresses the deflection via the converse piezoelectric effect. A finite element formulation is presented for static response of laminated shell with piezoelectric sensors/actuators. An eight-node and forty-DOF shell element is built. The performance of the shell elements is improved by reduced integration technique. The static shape control of structure is derived. The shell element is verified by calculating piezoelectric polymeric PVDF bimorph beam. The results agreed with those obtained by theoretical analysis, Tzou and Tseng (1990) and Hwang and Park (1993) fairly well. At last, the static shape control of a paraboloidal antenna is presented.

Key words: piezoelectric shell element; static shape control.

1. Introduction

Space structures, aircraft, and the like are required to be light in weight due to the high cost of transportation. Since they are also lightly damped, owing to the low internal damping of the materials used in their construction, the increased flexibility may allow large amplitude vibration and shape deformation, which may cause structural instability. These problems lead to a drastic reduction in accuracy and precision of operation. Thus, it is highly desirable to control excessive vibration and shape deformation and to stabilize the structure during operation (Ahmad *et al.* 1970, Zienkiewicz 1971).

Since the structures are, in general, distributed and flexible in nature, distributed dynamic measurement and active vibration suppression are essential to their performance. Vibration suppression and shape control of distributed parameter systems always represents a challenge in both theory and practice. Theoretical development has been constantly advanced in the past 20 years (Atluri and Amos 1988, Wada *et al.* 1989, Tzou 1988, 1989, Butkovskii 1962). However, due to the limitation of materials and actuator design, practical application of the theory to general distributed parameter systems still needs to be further explored. Besides, in order to control and suppress the undesirable structural oscillation and shape deformation of a distributed parameter system, an accurate measurement of the structural vibration is required. Conventional sensors are

† Professor
‡ Ph.D.
‡† Ph.D. Candidate

"discrete" in nature, i.e., measuring the response at spatially "discrete" locations. Some natural frequency and mode shapes could be missed if the sensors are placed at nodal modes or lines. Thus, the development of a "distributed" sensor can be essential for new-generation lightweight, high-performance structures. This paper is concerned with thin piezoelectric layers which are coupled with conventional materials and used as distributed sensors and distributed actuators in an intelligent advanced structure design.

The direct piezoelectric effect has been widely applied to variety of sensors designs. However, the converse piezoelectric effect is not common as compared with the direct effect. In this paper, the advanced structure is a shell configuration with one piezoelectric layer serving as a distributed sensor and the other layer serving as a distributed actuator. The direct effect is used in distributed sensing and the converse effect in distributed active vibration suppression and shape control of the advanced structure. Thus the sensing layer detects the oscillation of the distributed systems and the actuator controls the vibration or shape of the system. The piezoelectric material used in the finite element analysis of the advanced structures is PVDF or PZT (piezoceramics). Due to its distinct characteristics, such as flexibility, durability, manufacturability, etc. PVDF is an ideal material for the distributed sensing and vibration suppression/control of distributed parameter systems.

Up to now, research in this area has been primarily focused on experimental and theoretical study. General piezoelectric finite element development is relatively limited. In general, experimental models are limited by size, cost, and many other laboratory unknowns. Theoretical models can be more general, but analytical solutions are restricted to relatively simple geometries and boundary conditions (Tzou 1990). When the geometry and boundary conditions become relatively complicated, difficulties occur with both theoretical and experimental models. Thus, the finite element development becomes very important in modeling and analysis of advanced flexible structures with distributed piezoelectric sensors and/or actuators.

Before now, piezoelectiric beam elements (Im and Atluri 1989, Hwang and Park 1993), piezoelectric plate elements (Tiersten 1969), isoparametric hexahedron solid elements (Tzou 1990) and some shell elements (Kim *et al.* 1997 and Claeyssen *et al.* 2000) are developed. Those elements deal with the flat-shell structure or curve-shell structure with discrete sensors and actuators. The detail survey of piezoelectric elements is given in Benjeddou (2000). Although the general shell elements (Ahmad *et al.* 1970, Zhang *et al*. 1986, Crawley and Luis 1987, Gallayher 1969) have been studied in detail, the research of piezoelectric shell elements have just started for recent years. In order to study a paraboloidal antenna in controlling its shape and suppressing its oscillation, this paper presents an eight-node and forty-DOF isoparametric piezoelectric shell element in which the shear effects are considered. A finite element formulation is presented for modeling the static response of laminated shell structure containing distributed piezoelectric materials (PVDF) subjected to both mechanical and electrical load. The formulation is derived from the variational principle with consideration for the total potential energy of the structures and the electrical potential energy of the piezoelectric materials. The model is verified by calculating piezoelectric polymeric PVDF bimorph beam, and the results obtained agreed with those obtained by theoretical analysis fairly well.

2. Direct and converse piezoelectric effects

It is assumed that the mechanical and electrical forces in an oscillating piezoelectric structure are balanced at any given time instantly. Thus, the piezoelectric equations can be decoupled, i.e., a

quasi-static approximation is used in the analysis. It is also assumed that the temperature variation is negligible, The linear piezoelectric constitutive equations coupling the elastic and electric field can be respectively expressed as the direct and the converse piezoelectric equations (Tzou 1990):

$$\{D\} = [e]\{S\} + [\varepsilon^s]\{E\} \tag{1}$$

$$\{T\} = [C^E]\{S\} - [e]^T\{E\} \tag{2}$$

where $\{D\}$ is the electric displacement vector, $[e]$ is the dielectric permitivity matrix, $[e]^T$ is the transpose of $[e]$, $\{S\}$ is the strain vector, $[\varepsilon^s]$ is the dielectric matrix at constant or zero mechanical strain, $[E]$ is the electric field vector, $[T]$ is the stress vector, and $[C^E]$ is the elastic matrix for a constant or zero electric field.

3. A new piezoelectric finite element formulation

In this section, a thin piezoelectric shell element is studied by using a variational method and the principle of minimum potential energy. The system matrix equation is also formulated by assembling all of the element matrices.

3.1 Static finite element equations (Bathe 1982, Allik and Hughes 1979, Crawley and Luis 1987)

Consider a piezoelectric shell element with eight nodes as shown in Fig. 1. Each node has five DOFs, 3 transitional and 2 rotational. $o\xi\eta\zeta$ is a natural coordinate system, ξ and η are curve coordinates of middle surface of shell. The surface (ζ=1) is defined as top one; the surface ($\zeta = -1$) is defined as bottom one. Eight nodes are on the middle surface (Fig. 1). Through each node, a normal line is drawn, the normal line intersects with the top and bottom surface. The intersection points are called correspondent nodes. The top and bottom surface are actuator and sensor layer respectively.

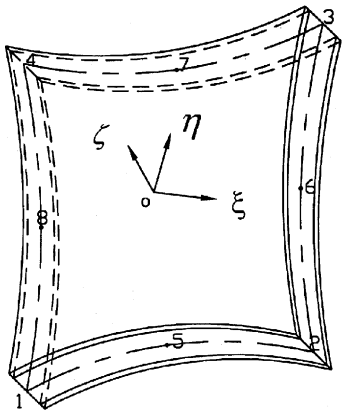

Fig. 1 A piezoelectric shell element

3.1.1 Coordinate transformation

The nodal coordinates of the element are:

$$\begin{Bmatrix} x_i \\ y_i \\ z_i \end{Bmatrix}_{\text{middle}} = \frac{1}{2}\left(\begin{Bmatrix} x_i \\ y_i \\ z_i \end{Bmatrix}_{\text{top}} + \begin{Bmatrix} x_i \\ y_i \\ z_i \end{Bmatrix}_{\text{bottom}} \right) \tag{3}$$

The normal vector of surface at the *i*th node is defined as:

$$\vec{V}_{3i} = \begin{Bmatrix} l_{3i} \\ m_{3i} \\ n_{3i} \end{Bmatrix} = \frac{1}{h_i}\left(\begin{Bmatrix} x_i \\ y_i \\ z_i \end{Bmatrix}_{\text{top}} - \begin{Bmatrix} x_i \\ y_i \\ z_i \end{Bmatrix}_{\text{bottom}} \right) \tag{4}$$

where $h_i = \sqrt{(x_{i\text{top}} - x_{i\text{bottom}})^2 + (y_{i\text{top}} - y_{i\text{bottom}})^2 + (z_{i\text{top}} - z_{i\text{bottom}})^2}$ is the thickness of the element.

The global coordinates of any point on the normal line of the *i*th node is:

$$\begin{Bmatrix} x_i \\ y_i \\ z_i \end{Bmatrix} + \frac{h_i}{2}\zeta\vec{V}_{3i} \qquad (i = 1, 2, \cdots, 8) \tag{5}$$

The global coordinates of any point in the element is:

$$\begin{Bmatrix} x \\ y \\ z \end{Bmatrix} = \sum_{i=1}^{8} N_i(\xi,\eta)\left(\begin{Bmatrix} x_i \\ y_i \\ z_i \end{Bmatrix} + \frac{h_i}{2}\zeta\vec{V}_{3i} \right) \tag{6}$$

where

$$\begin{aligned} N_i(\xi,\eta) = {} & (1+\xi_0)(1+\eta_0)(\xi_0+\eta_0-1)\xi_i^2\eta_i^2/4 \\ & + (1-\xi^2)(1+\eta_0)(1-\xi_i^2)\eta_i^2/2 \\ & + (1-\eta^2)(1+\xi_0)(1-\eta_i^2)\xi_i^2/2 \end{aligned} \tag{7}$$

where

$$\xi_0 = \xi_i\xi \qquad \eta_0 = \eta_i\eta \qquad (i = 1, 2, \cdots, 8) \tag{8}$$

Now, apply the interpolation method to establish a local coordinate system of the element, i.e., $o'x'y'z'$. Three axis vectors can be expressed as:

$$\vec{V}_3 = \begin{Bmatrix} l_3 \\ m_3 \\ n_3 \end{Bmatrix} = \frac{\sum_{i=1}^{8} N_i\vec{V}_{3i}}{\left|\sum_{i=1}^{8} N_i\vec{V}_{3i}\right|} \tag{9}$$

$$\vec{V}_1 = \begin{Bmatrix} l_1 \\ m_1 \\ n_1 \end{Bmatrix} = \frac{\vec{i} \times \vec{V}_3}{|\vec{i} \times \vec{V}_3|} \tag{10}$$

$$\vec{V}_2 = \begin{Bmatrix} l_2 \\ m_2 \\ n_2 \end{Bmatrix} = \vec{V}_3 \times \vec{V}_1 \tag{11}$$

Therefore, coordinate transformation matrix between *oxyz* and $o'x'y'z'$ is:

$$[\theta] = [\vec{V}_1 \ \vec{V}_2 \ \vec{V}_3] = \begin{bmatrix} l_1 & l_2 & l_3 \\ m_1 & m_2 & m_3 \\ n_1 & n_2 & n_3 \end{bmatrix} \tag{12}$$

Transformation matrix of strain tensor can be expressed as:

$$[T_w] = \begin{bmatrix} l_1^2 & m_1^2 & n_1^2 & l_1 m_1 & m_1 n_1 & n_1 l_1 \\ l_2^2 & m_2^2 & n_2^2 & l_2 m_2 & m_2 n_2 & n_2 l_2 \\ 2l_1 l_2 & 2m_1 m_2 & 2n_1 n_2 & l_1 m_2 + l_2 m_1 & m_1 n_2 + m_2 n_1 & n_1 l_2 + n_2 l_1 \\ 2l_2 l_3 & 2m_2 m_3 & 2n_2 n_3 & l_2 m_3 + l_3 m_2 & m_2 n_3 + m_3 n_2 & n_2 l_3 + n_3 l_2 \\ 2l_3 l_1 & 2m_3 m_1 & 2n_3 n_1 & l_3 m_1 + l_1 m_3 & m_3 n_1 + m_1 n_3 & n_3 l_1 + n_1 l_3 \end{bmatrix} \tag{13}$$

where it is assumed that a line segment on the normal line in the local coordinate system doesn't both extend and contract.

3.1.2 Displacement model

The other axis vectors which are vertical to $\vec{V}_{3i}$ are defined as:

$$\vec{V}_{1i} = \begin{Bmatrix} l_{1i} \\ m_{1i} \\ n_{1i} \end{Bmatrix} = \frac{\vec{i} \times \vec{V}_{3i}}{|\vec{i} \times \vec{V}_{3i}|} \tag{14}$$

$$\vec{V}_{2i} = \frac{\vec{V}_{3i} \times \vec{V}_{1i}}{|\vec{V}_{3i} \times \vec{V}_{1i}|} = \vec{V}_{3i} \times \vec{V}_{1i} \tag{15}$$

where

$$\vec{i} = \begin{Bmatrix} 1 \\ 0 \\ 0 \end{Bmatrix} \tag{16}$$

The displacements of any point on the normal line of the *i*th node are calculated by motion formulation.

$$\begin{Bmatrix} u_i \\ v_i \\ w_i \end{Bmatrix} + \vec{\omega}_i \times \frac{h_i}{2}\zeta\vec{V}_{3i} = \begin{Bmatrix} u_i \\ v_i \\ w_i \end{Bmatrix} + \frac{h_i}{2}\zeta[\vec{V}_{1i} - \vec{V}_{2i}]\begin{Bmatrix} \alpha_i \\ \beta_i \end{Bmatrix} \tag{17}$$

where β_i and α_i are the angle of rotation that $\vec{V}_{3i}$ rotates about $\vec{V}_{1i}$ and $\vec{V}_{2i}$, $\vec{\omega}_i = \beta_i\vec{V}_{1i} + \alpha_i\vec{V}_{2i}$ is rotational vector, u_i, v_i and w_i are the displacements of the *i*th node, $\vec{\omega}_i \times h_i/2\,\zeta\vec{V}_{3i}$ is the displacement caused by rotation. Therefore, the displacement of any point in the element can be expressed as:

$$\begin{Bmatrix} u \\ v \\ w \end{Bmatrix} = \sum_{i=1}^{8} N_i(\xi,\eta)\left(\begin{Bmatrix} u_i \\ v_i \\ w_i \end{Bmatrix} + \zeta[\psi_i]\begin{Bmatrix} \alpha_i \\ \beta_i \end{Bmatrix}\right) \tag{18}$$

where

$$[\psi_i] = \begin{bmatrix} \psi_{11i} & \psi_{12i} \\ \psi_{21i} & \psi_{22i} \\ \psi_{31i} & \psi_{32i} \end{bmatrix} = \frac{h_i}{2}[\vec{V}_{1i}\ \vec{V}_{2i}] \tag{19}$$

The Eq. (18) can be rewritten as:

$$\begin{Bmatrix} u \\ v \\ w \end{Bmatrix} = [N]\begin{bmatrix} \delta_1^e \\ \delta_2^e \\ \vdots \\ \delta_8^e \end{bmatrix} = \sum_{i=1}^{8}[N_i][\delta_i^e] \tag{20}$$

where

$$[\delta_i^e] = [u_i\ v_i\ w_i\ \alpha_i\ \beta_i]^T \tag{21}$$

$$[N_i] = N_i[I \quad \zeta\psi_i] \tag{22}$$

where $[I]$ is three-order unit matrix.

3.1.3 Finite element equations

To derive the finite element equation of each element, the element displacement $\{u\ v\ w\}^T$ and electric potential ϕ_s, ϕ_a are defined in terms of nodal variables via the shape function matrices $[N]$ and $[N_s]$, $[N_a]$ (Bathe 1982, Ahmad *et al.* 1970, Crawley and Luis 1987, Gallayher 1969).

$$\begin{Bmatrix} u \\ v \\ w \end{Bmatrix} = [N]\{\delta^e\} = \sum_{i=1}^{8}[N_i][\delta_i^e] \tag{23}$$

$$\phi_s = [N_s]\{\phi_s^e\} \qquad \phi_a = [N_a]\{\phi_a^e\} \tag{24}$$

where

$$\{\phi_s^e\} = \{\phi_{s1}, \phi_{s2}, \ldots, \phi_{s8}\}^T \tag{25}$$

$$\{\phi_a^e\} = \{\phi_{a1}, \phi_{a2}, \ldots, \phi_{a8}\}^T \tag{26}$$

$$[N_s] = [N_a] = [N_1, N_2 \ldots, N_8] \tag{27}$$

Although $[N_s]$ and $[N_a]$ are of the same formulation, their domains are not the same. ϕ_{si} and ϕ_{ai} ($i = 1, 2, \cdots, 8$) are nodal electrical potentials of the top and bottom surface respectively. The strain vector $\{S\}$ are defined by the first partial derivative of nodal displacement vector $\{u\ v\ w\}^T$ by using a differential operator matrix:

$$\{S\} = \begin{Bmatrix} \dfrac{\partial u}{\partial x} \\ \dfrac{\partial v}{\partial y} \\ \dfrac{\partial w}{\partial z} \\ \dfrac{\partial u}{\partial y} + \dfrac{\partial v}{\partial x} \\ \dfrac{\partial w}{\partial y} + \dfrac{\partial v}{\partial z} \\ \dfrac{\partial w}{\partial x} + \dfrac{\partial u}{\partial z} \end{Bmatrix} = \sum_{i=1}^{8} [B_i]\{\delta_i^e\} = [B]\{\delta^e\} \tag{28}$$

The stress vector $\{T\}$ can be calculated by following formulation

$$\{T\} = [C]\{S\} \tag{29}$$

where stiffness matrix $[C]$ is not of simple style, and can be obtained by coordinate transformation. The transformation formulation is:

$$[C] = [T_\omega]^T [C'][T_\omega] \tag{30}$$

where

$$[C'] = \frac{E'}{1-\mu^2} \begin{bmatrix} 1 & \mu & 0 & 0 & 0 \\ \mu & 1 & 0 & 0 & 0 \\ 0 & 0 & \dfrac{1-\mu}{2} & 0 & 0 \\ 0 & 0 & 0 & \dfrac{1-\mu}{2} & 0 \\ 0 & 0 & 0 & 0 & \dfrac{1-\mu}{2} \end{bmatrix} \tag{31}$$

where E' is the Young's modulus; μ is the Poisson's ratio.

The electric field vector $\{E\}$ is defined by the negative gradient of the potential:

$$\{E_a\} = -\nabla\phi_a = -\sum_{i=1}^{8} B_{\phi_i}\phi_{a_i}^e = -[B_{a\phi}]\{\phi_a^e\} \tag{32}$$

$$\{E_s\} = -\nabla\phi_s = -\sum_{i=1}^{8} B_{\phi_i}\phi_{s_i}^e = -[B_{s\phi}]\{\phi_s^e\} \tag{33}$$

where

$$\{B_{\phi_i}\} = \left[\frac{\partial N_i}{\partial x}, \frac{\partial N_i}{\partial y}, \frac{\partial N_i}{\partial z}\right]^T \qquad (i = 1, 2, \cdots, 8) \tag{34}$$

The finite element equations of the element can be derived by the principle of minimum potential energy

$$\delta[(U_m + U_a + U_s) - (W_m + W_a + W_s)] = 0 \tag{35}$$

where

$$U_m = \int_{V_m} \frac{1}{2}\left(\{S_m\}^T\{T_m\} - \{E_m\}^T\{D_m\}\right)dv \tag{36}$$

$$U_a = \int_{V_a} \frac{1}{2}\left(\{S_a\}^T\{T_a\} - \{E_a\}^T\{D_a\}\right)dv \tag{37}$$

$$U_s = \int_{V_s} \frac{1}{2}\left(\{S_s\}^T\{T_s\} - \{E_s\}^T\{D_s\}\right)dv \tag{38}$$

$$W_m = \int_s \{U\}^T\{P_s\}ds + \{U\}^T\{P_c\} \tag{39}$$

$$W_a = -\int_{S_a} \phi_a\sigma_a\, ds_a \tag{40}$$

$$W_s = -\int_{S_s} \phi_s\sigma_s\, ds_s \tag{41}$$

where subscript m, a, s denotes the main structure, actuator layer and sensor layer respectively. In Eqs. (36)–(38), $\{S_m\}$, $\{S_a\}$ and $\{S_s\}$ are similar to $\{S\}$ of Eq. (28), $\{T_a\}$ and $\{T_s\}$ are similar to Eq. (2), but their domains of integration are not the same; $\{T_m\}$ is the same as $\{T\}$; $\{E_m\}$ and $\{D_m\}$ are zero vectors; $\{D_a\}$ and $\{D_s\}$ are similar to $\{D\}$ in Eq. (1); V_m, V_a and V_s are the domains of integration of three layers, respectively; $\{U\}$ is the displacement; $\{P_s\}$ is the distributed load of the element; $\{P_c\}$ is the concentrated load; ϕ_a and ϕ_s are potentials; σ_a and σ_s are the surface charge density of the top and bottom layers.

Substituting Eqs. (36)–(41) into (35) yields the finite element equation of the element:

$$\left([K_{mm}^e] + [K_{aa}^e] + [K_{ss}^e]\right)\{\delta^e\} + [K_{aa\phi}^e][\phi_a^e] + [K_{ss\phi}^e][\phi_s^e] = \{F^e\} \tag{42}$$

$$[K_{a\phi a}^e]\{\delta^e\} - [K_{a\phi a\phi}^e]\{\phi_a^e\} = \{G_a^e\} \tag{43}$$

$$[K_{s\phi s}^e]\{\delta^e\} - [K_{s\phi s\phi}^e]\{\phi_a^e\} = \{G_s^e\} \tag{44}$$

where

$$[K_{mm}^e] = \int_{V_m} [B_m^e]^T [C_m][B_m^e] dv \tag{45}$$

$$[K_{aa}^e] = \int_{V_a} [B_a^e]^T [C_a][B_a^e] dv \tag{46}$$

$$[K_{ss}^e] = \int_{V_s} [B_s^e]^T [C_s][B_s^e] dv \tag{47}$$

$$[K_{aa\phi}^e] = \int_{V_a} [B_a^e]^T [e]^T [B_{a\phi}^e] dv \tag{48}$$

$$[K_{a\phi a\phi}^e] = \int_{V_a} [B_{a\phi}^e]^T [\varepsilon][B_{a\phi}^e] dv \tag{49}$$

$$[K_{a\phi a}^e] = [K_{aa\phi}^e]^T \tag{50}$$

$$[K_{ss\phi}^e] = \int_{V_s} [B_s^e]^T [e]^T [B_{s\phi}^e] dv \tag{51}$$

$$[K_{s\phi s\phi}^e] = \int_{V_s} [B_{s\phi}^e]^T [\varepsilon][B_{s\phi}^e] dv \tag{52}$$

$$[K_{s\phi s}^e] = [K_{ss\phi}^e]^T \tag{53}$$

$$\{F^e\} = \int_s [N]^T [P_s] ds + [N]^T [P_c] \tag{54}$$

$$\{G_a^e\} = -\int_{s_a} [N_a]^T \sigma_a ds \tag{55}$$

$$\{G_s^e\} = -\int_{s_s} [N_s]^T \sigma_s ds \tag{56}$$

where $[B_m^e]$, $[B_a^e]$ and $[B_s^e]$ are of the same formulations, only their domains are not the same; $[B_{a\phi}^e]$ and $[B_{s\phi}^e]$ are of the same formulations, but their domains are not the same; $[C_m]$, $[C_a]$ and $[C_s]$ are the elastic constant matrices of the main, actuator and sensor, respectively. By the coordinate transformation and the Gauss' integration, the integral calculations of the stiffness matrices can be completed. Because the element is the thin shell, it suffers from the locking phenomena. In order to overcome the shortcomings, the reduced integration technique (Ahmad *et al.* 1970, Zienkiewicz *et al*. 1971) is applied to improve the performance of the element, which can assure that it is convergent.

It should be noted that $[e]$ and $[\varepsilon]$ are not the same as those of plane beams and plate elements. In plane beam and plate elements, they are constant matrices, but now they are two-order tensors for the shell element. Calculating them needs tensor transformation. The tensor transformation formula are as follows

$$[\varepsilon] = [\theta][\varepsilon'][\theta]^T \tag{57}$$

$$[e] = [\theta][e'][T_\omega] \tag{58}$$

where

$$[\varepsilon] = \begin{bmatrix} \varepsilon'_{11} & 0 & 0 \\ 0 & \varepsilon'_{22} & 0 \\ 0 & 0 & \varepsilon'_{33} \end{bmatrix} \tag{59}$$

$$[e'] = \begin{bmatrix} 0 & 0 & 0 & e'_{14} & 0 \\ 0 & 0 & e'_{23} & 0 & 0 \\ e'_{31} & e'_{32} & 0 & 0 & 0 \end{bmatrix} \tag{60}$$

The material properties can be found in Tzou and Tseng (1990).

3.2 Condensation of electrical potential matrix (Xie and He 1981)

In the distributed sensing and vibration suppression analysis, the displacements is much more important than the electrical potential vector in most applications. In order to save computer memory and improve computation efficiency, the electrical potential vector is usually condensed in the time domain integration. However, a recovery scheme can be set up if the sensing information is required. From Eqs. (43)–(44) $\{\phi_a^e\}$, $\{\phi_s^e\}$ can be calculated as

$$\{\phi_a^e\} = [K_{a\phi a\phi}^e]^{-1}\left([K_{a\phi a}^e]\{\delta^e\} - \{G_a^e\}\right) \tag{61}$$

$$\{\phi_s^e\} = [K_{s\phi s\phi}^e]^{-1}\left([K_{s\phi s}^e]\{\delta^e\} - \{G_s^e\}\right) \tag{62}$$

Substituting Eqs. (61), (62) into Eq. (42) yields the finite element equation.

$$[K^e]\{\delta^e\} = [F^e] + [F_a^e] + [F_s^e] \tag{63}$$

where

$$[K^e] = [K_{mm}^e] + [K_{aa}^e] + [K_{ss}^e] + [K_{aa\phi}^e][K_{a\phi a\phi}^e]^{-1}[K_{a\phi a}^e] + [K_{ss\phi}^e][K_{s\phi s\phi}^e]^{-1}[K_{s\phi s}^e] \tag{64}$$

$$\{F_a^e\} = [K_{aa\phi}^e][K_{a\phi a\phi}^e]^{-1}\{G_a^e\} \tag{65}$$

$$\{F_s^e\} = [K_{ss\phi}^e][K_{s\phi s\phi}^e]^{-1}\{G_s^e\} \tag{66}$$

In the above equations, $\{F^e\}$ is the external mechanical excitation and $\{F_a^e\}$, $\{F_s^e\}$ is the electrical excitation respectively. In Eq. (62), $\{\phi_s^e\}$ is the electrical potential output of the sensor. Note that $\{G_s^e\}$ is usually zero in the distributed sensor layer. Thus, the electrical potential output of the distributed sensor is estimated by

$$\{\phi_s^e\} = [K_{s\phi s\phi}^e]^{-1}([K_{s\phi s}^e]\{\delta^e\}) \tag{67}$$

In the active control application, $\{\phi_s^e\}$ is the feedback voltage determined by the control algorithm.

The structural static equation can be written as follows:

$$[K]\{\delta\} = \{F\} + \{F_a\} + \{F_s\} \tag{68}$$

4. Numerical example

Because there are not analytic and experimental results regarding the piezoelectric shell element in

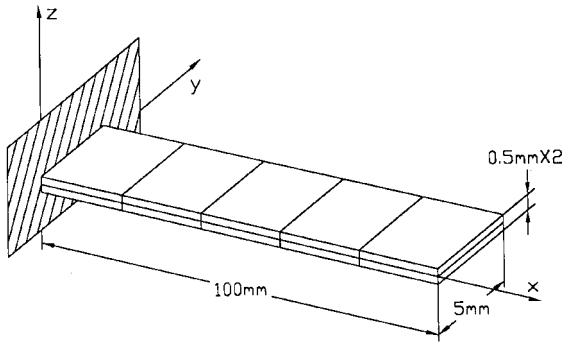

Fig. 2 A piezoelectric polymeric PVDF bimorph beam

the open literature, the piezoelectric bimorph beam (Tzou 1990) is only studied to verify the model. The structure was made of two layers of piezoelectric polymeric PVDF with opposite polarity. When an external voltage is applied, the induced internal stresses result in a bending moment which forces the bimorph beam to bend. The first study was a static deflection case in which a voltage was applied across the thickness and the beam deflection was studied by using the above model. The second study was that the distributed voltage along the beam was calculated, when the tip of the beam has a load. The bimorph beam model was discretised into ten piezoelectric finite elements, five elements on each layer, one end of the bimorph beam was assumed fixed. The material properties of PVDF can be found in Tzou and Tseng (1990). The physical dimension and polarity are illustrated in Fig. 2.

4.1 Static deflection (the converse effect)

A unit voltage (1V) was applied across the thickness and the static deflections of five nodes were calculated analytically (Hwang and Park 1993) and by the finite element method. The calculated deflections are compared with those obtained by Tzou (1990) and theoretical solutions in Fig. 3.

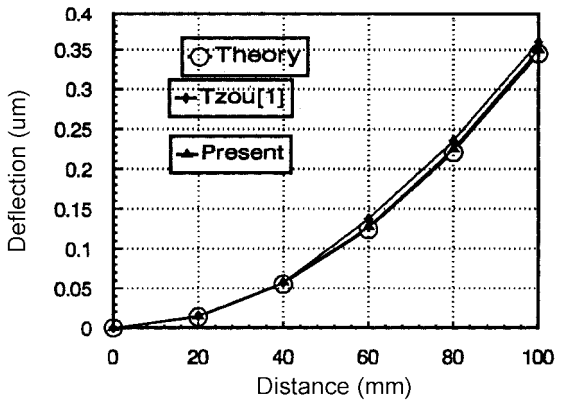

Fig. 3 Deflection of the piezoelectric PVDF bimorph beam (voltage input = 1V)

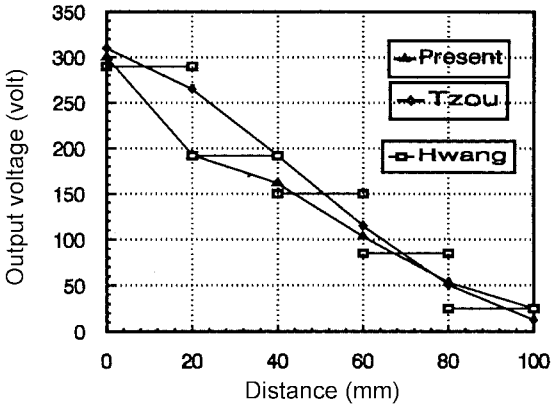

Fig. 4 Sensor voltage distribution for the bending deflection

From Fig. 3, it can be seen that the present finite element solutions agree with those obtained by the theoretical analysis fairly well. The present finite element solutions are better than those obtained by Tzou and Tseng (1990).

4.2 Distributed structural identification (the direct effect)

The piezoelectric bimorph beam was also studied for its voltage response, when an initial tip load of 0.12 N (which produces the tip deflection of about 1 cm) was performed, and the voltage response was calculated by using the present finite element method. Because the direct effects of the bimorph beam does not have theoretical solutions, the results can only compare with those of Tzou and Tseng (1990) and Hwang and Park (1993) in Fig. 4. From the results obtained by the present model agreed with those obtained by Tzou and Tseng (1990) and Hwang and Park (1993).

5. The static shape control for the intelligent structure (Shi and Atluri 1990, Chen *et al.* 1997)

The load term of Eq. (63) contains three terms, i.e., the mechanical force $\{F^e\}$, the electrical forces $\{F_a^e\}$ and $\{F_s^e\}$. When no external electrical field is performed on the sensors, $\{F_s^e\}$ is zero vector. By using Eqs. (55) and (65), $\{F_a^e\}$ can be obtained (Xie and He 1981)

$$\begin{aligned}\{F_a^e\} &= [K_{aa\phi}^e][K_{a\phi a\phi}^e]^{-1}\{G_a^e\} \\ &= -[K_{aa\phi}^e][K_{a\phi a\phi}^e]^{-1}\int_{S_a}[N_a]^T\sigma_a ds \\ &= -[K_{aa\phi}^e][K_{a\phi a\phi}^e]^{-1}\frac{\varepsilon_0}{h_a}\{V_a^e\}\end{aligned} \tag{69}$$

where ε_0 is the absolute permitivity, h_a the thickness of the actuator and $\{V_a^e\}$ the nodal electrical voltage in the actuator. It is concluded that changing the electrical voltage input to the distributed actuators can change electrical forces. Further, if mechanical forces are constant, the change of the electrical voltage input to the actuators will cause the change of the nodal displacements. Therefore, it is possible to control the shape of the structure with distributed piezoelectric S/As by changing the electrical voltage input to the actuators. $\{F_a^e\}$ can be regarded as the control forces.

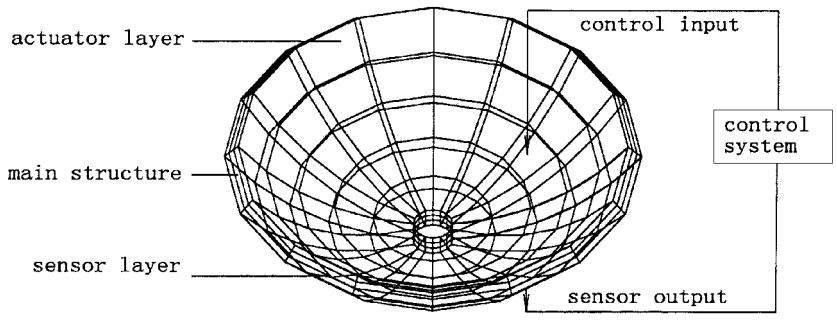

Fig. 5 The active control system of an intelligent shell structure

The basic configuration of an intelligent structure is composed of the main structure sandwiched between two piezoelectric thin layers. If one of the piezoelectric thin layer is acted as the distributed sensors and other the actuators, and a feedback control law is implemented by the control system, then the shape of the structure can be controlled actively.

An active control system of a shell structure with piezoelectric materials, in which the bottom is acted as distributed sensors and the top as distributed actuators, is shown in Fig. 5.

In the active control, if the mechanical forces are applied to the structure, the sensor outputs electrical potential expressed by Eq. (67). The electrical potential is then amplified by the feedback gain through a feedback control circuit and feedback to the actuator as the applied electrical voltage. Thus,

$$\{V_a^e\} = G\{\phi_s^e\} \tag{70}$$

where G is a feedback gain. Then the actuators generate counteracting motion to control the shape of the structure. Now the finite element equation for the shape control of the intelligent structure becomes

$$\left([K^e]+\frac{\varepsilon_0}{h_a}G[K_{aa\phi}^e][K_{a\phi a\phi}^e]^{-1}[K_{s\phi s\phi}^e]^{-1}[K_{s\phi s}^e]\right)\{\delta^e\} = \{F^e\} \tag{71}$$

By solving this equation, the displacements of nodes with active control can be obtained. The feedback gain G is adjusted until the desired shape of the structure has been reached.

6. Static shape control of a paraboloidal antenna

In this section, as the application of the piezoelectric shell element presented in the above, we consider the static shape control of the paraboloidal antenna (Fig. 6).

6.1 Model definition

The shell structure (diameter: 1 m; thickness: 2 mm; height: 100 mm; ρ = 2.68 E3; E = 8.0 E9; μ= 0.28) with a distributed piezoelectric PVDF (material property can be found in Hwang and Park 1993, Atluri and Amos 1988) layer (0.5 mm) serving as a distributed actuator on the top surface, and another PVDF (0.1 mm) on the bottom surface as a distributed sensor, was studied. The structure was divided into 240 elements, 80 for each layer. The bottom boundary nodes of the structure are simply supported. In the computation of the integration, when $3\times3\times3$ or higher order Gauss' integration is applied to compute the integration, the locking phenomena occurs, but the $2\times2\times2$ Gauss' integration is applied, the locking phenomena is improved. Therefore, the reduced integration technique can assure the shell element is convergence.

6.2 Static shape control

When the external loads P_k (P_k = –1000 N, k = 0, 2, 4, ⋯, 14) were applied on nodes of which the cylindrical coordinates are ((0.4, $0.3927\times k$, 0.064), k = 0, 2, 4, ⋯, 14), the deflection of the structure is shown as in Fig. 7.

The surface with solid line denotes original structure, and the surface with dashed line denotes the

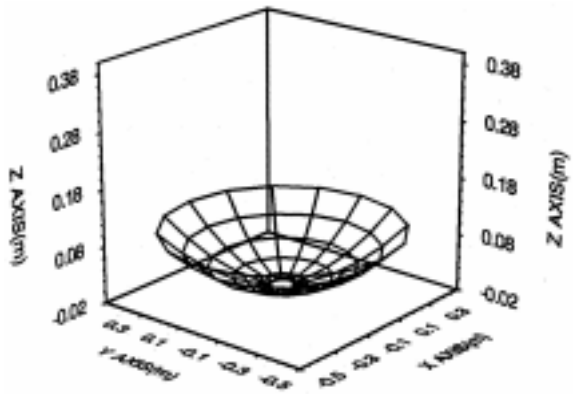

Fig. 6 Finite element modeling of the shell structure with distributed piezoelectric sensor/actuator

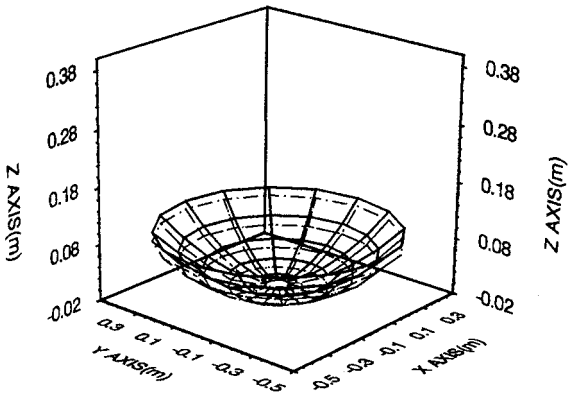

Fig. 7 Static deflection of the structure

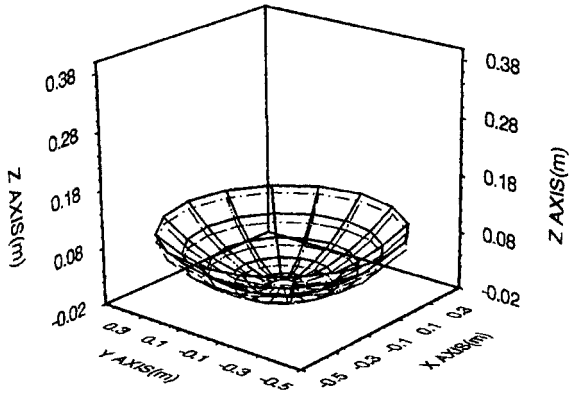

Fig. 8 Control effect of G=100

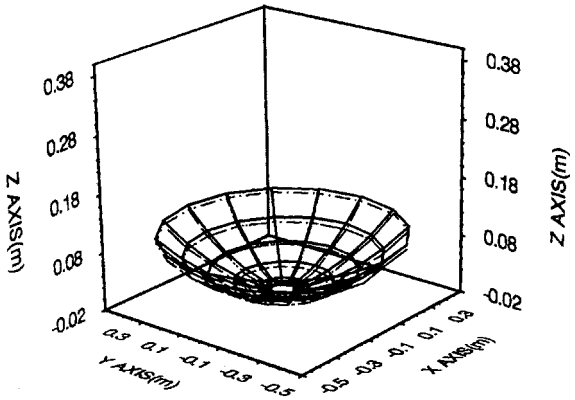

Fig. 9 Control effect of G=500

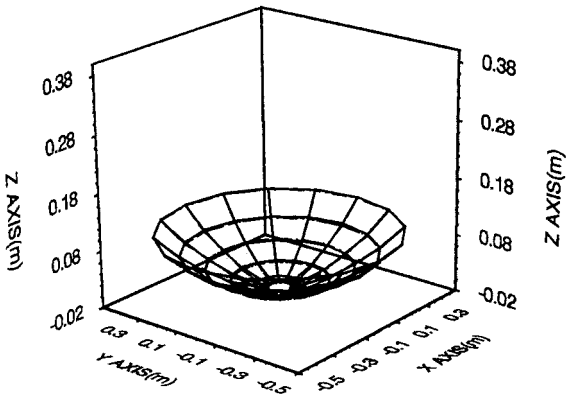

Fig. 10 Control effect of G=900

deformed structure. By section 5, when G is equals to 100, 500, 900, respectively, the control results are as those of Figs. 8–10.

It can be seen that, when $G=900$, the controlled structure is almost coincident with the original structure.

7. Conclusions

A new three-dimensional piezoelectric thin shell element containing an integrated distributed piezoelectric sensor and actuator is built. All formulations are derived. The present shell element is applied to not only flat-shell structure but also curve-shell structure. It can be applied to shape, oscillation and noise controlling of the plate and shell structures. The relevant finite element program is accomplished. The numerical results of the antenna shows that the shell element presented in this paper is valid for static shape controlling of the shell structures. It is also applied to dynamic shape controlling which is our next task.

Acknowledgements

This project was supported by the National Natural Science Foundation of China. The authors are grateful to Dr. Cheng Huang, Dr. Zhong-dong Wang and Dr. Wan-zhi Han and both reviewers for their helpful suggestions and discussions.

References

Ahmad, S., Irons, B.M., and Zienkiewicz, O.C. (1970), "Analysis of thick and thin shell structure by curved elements", *Int. J. Numer. Meth. in Eng.*, **2**, 419-451.

Allik, H., and Hughes, T.J. (1979), "Finite element method for piezoelectric vibration", *Int. J. Numer. Meth. in Eng.*, **2**, 151-168.

Atluri, S.N., and Amos, A.K. (1988), *Large Space Structures: Dynamics and Control*, Springer-verlag, Berlin.

Bathe, K.J. (1982), *Finite Element Procedures in Engineering Analysis*, Prentice-Hall, Inc., Englewood Cliffs, New Jersey.

Benjeddou, A. (2000), "Advances in piezoelectric finite element modeling of adaptive structural elements: A survey", *Comput. and Struct*., **76**(1), 347-363.

Butkovskii, A.G. (1962), "The maximum principle for optimum systems with distributed parameters", *Automation and Remote Control*, **22**, 1429-1438.

Chen, S.H., Wang, Z.D., and Liu, X.H. (1997), "Active vibration cotrol and suppression for intelligent structures", *J. Sound and Vibration*, **200**(2), 167-177.

Claeyssen, F., Lherment, N., Le Letty, R., Barillot, F., Debarnot, M., Six, M.F., Thomin, G., and Privat, M. (2000), *Proc. of SPIE - The International Society for Optical Engineering 3991 Mar 7 - Mar 9 2000* Sponsored by: SPIE Society of Photo -- Optical Instrumentation Engineers, 202-209.

Crawley, E.F., and Luis, J. (1987), "Use of piezoelectric actuators as elements of intelligent structures", *American Inst. of Aeronaut. and Astronaut. J*., **25**(10), 1373-1385.

Gallayher, R.H. (1968), "Analysis of plate and shell structures", *Applications of Finite Element Method in Engineering*, Vanderbilt Univ., ASCE. 155-205.

Guyan, R.J. (1965), "Reduction of stiffness and mass matrixes", *AIAA J.*, **3**(2), 380-386.

Im, S., and Atlurim, S.N. (1989), "Effects of a piezo-actuator on a finitely deformed beam subjected to general

loading", *AIAA J.*, **27**(12), 1801-1807.
Kim Jaehwan, Waradan, V.V., and Varadan, V.K. (1997), "Finite element modeling of structures including piezoelectric active devises", *Int. J. Numer. Meth. in Eng.*, **40**(5), 817-832.
Shi, G., and Atluri, S.N. (1990), "Active control of nonlinear dynamic response of space-frames using piezo-electric actuators", *Comput. & Struct.*, **34**(4), 549-564.
Tiersten, H.F. (1969), *Linear Piezoelectric Plate Vibrations*, New York: Plenum Press.
Tzou, H.S. (1988), "Integrated sensing and adaptive vibration suppression of distributed systems", *1988 Recent Developments in Control of Nonlinear and Distributed Parameter Systems*, ASME-DSC, **10**, 51-58.
Tzou, H.S. (1989), "Development of a light-weight robot end-effector using polymeric piezoelectric bimorph", *Proc. of the 1989 IEEE Int. Conf. on Robotics and Automation (Scottsdale, AZ)*, Computer Society Press, Los Angeles, CA. **14-19**, May, 1704-1709.
Tzou, H.S., and Tseng, C.I. (1990), "Distributed piezoelectric sensor/actuator design for dynamic measurement/ control of distributed parameter systems: A piezoelectric finite element approach", *J. Sound and Vibration*, **138**(1), 17-34.
Wada, B.K., Fanson, J.l., and Crawley, E.F. (1989), "Adaptive structures", *Adaptive Structures*, ed. by Wada, B. K., ASME, New York, 1-8.
Woo-Seok Hwang and Hyun Chul Park (1993), "Finite element modeling of piezoelectric sensors and actuators", *AIAA J.*, **31**(5), 930-937.
Xie, Y.Q., and He, F.B. (1981), *A Finite Element Method in Elastic and Plastic Mechanics*, Machine Industry Press, China.
Zhang, J.D., O'Donoghue, P.E., and Atluri, S.N. (1986), "Analysis and control of finite deformations of plates and shells", *Finite Element Methods for Plate and Shell Structure*, Chapter 6, T. T. R. Hughes and E. Hinton, eds., Pineridge Press, Swansea, 127-153.
Zienkiewicz, O.C., Too, T., and Taylor, R.L. (1971), "Reduced integration technique in general analysis of plates and shells", *Int. J. Numer. Meth. in Eng.*, **3**, 275-290.